Quantum Information and Computation, Vol. 24, No. 5&6 (2024) 0425–0437


# ESTIMATING PI USING HIGH-DIMENSIONAL SINGLE AND MULTI-GLOBAL QUANTUM PHASE ESTIMATION ALGORITHM ON CIRQ

OSMAN SEMİ CEYLAN[a]
*Department of Computer Engineering, Çanakkale Onsekiz Mart University*
*Çanakkale, 17020, Türkiye*

SABRİ GÜNDÜZ
*Department of Physics, Faculty of Sciences, Çanakkale Onsekiz Mart University*
*Çanakkale, 17020, Türkiye*

*Department of Mathematics, School of Graduate Studies, Çanakkale Onsekiz Mart University*
*Çanakkale, 17020, Türkiye*

FURKAN KAYA
*Department of Computer Engineering, Çanakkale Onsekiz Mart University*
*Çanakkale, 17020, Türkiye*

İHSAN YILMAZ
*Department of Computer Engineering, Çanakkale Onsekiz Mart University*
*Çanakkale, 17020, Türkiye*

Received January 15, 2024
Revised April 18, 2024

Quantum computing is carried out based on the working principles of quantum mechanics. Current 2-dimensional quantum computing techniques face major problems such as noise and information capacity. As such, high-dimensional quantum computing is leveraged to solve these problems. This study attempts to approximate the pi number through the multi-global and single-global Quantum Phase Estimation (QPE) algorithms in high-dimension. This study reveals that pi can be calculated by using fewer quantum resources in high dimension with at least equal or higher precision than that obtained by 2-dimensional QPE. In addition, when the number of qudits or the number of dimensions is kept constant, the multi-global QPE in high dimensions yields at least equal or better results than the single-global QPE. All calculations performed in this study are implemented on Cirq.

*Keywords*: Pi, Quantum Computation, High-Dimension

*Communicated by*: to be filled by the Editorial

## 1 Introduction

Numerical approximation calculations are one of the mathematical methods to calculate the approximate value of a number [1, 2]. These calculations are based on the iterative approach of a set of operations depending on the input parameter that changes at each step to the value

[a]Corresponding author. E-mail: osman.semi.ceylan@gmail.com

to be approximated. Examples of these calculations were previously performed by Newton-Raphson [3], Divide and Conquer [4], Convergent Series [5], and Monte-Carlo [6]. These algorithms are widely applied in different areas such as engineering, finance, statistics, and physics [7, 8]. These convergence methods and their variations are encoded as algorithms that can be run by semiconductor-based processors, which developed rapidly in the 20th century, or today's classical computers [9]. Numerical solution methods are also encoded in devices known as quantum computers [10].

Quantum computers are devices that can perform calculations using quantum mechanical principals such as superposition and entanglement. The idea of such a device was originally put forward by Richard Feynman [11]. Later based on his idea, experimental quantum computers were developed [12, 13, 14, 15]. The superiority of quantum computers over the classical ones in performance criteria, including speed in running an algorithm, storage, and security, has been proved by Grover Search Algorithm [16], Deutsch [17], Deutsch-Jozsa [18] and Shor's prime factorization [19] algorithm. The superiority of quantum computing [20] has been shown also by Google. Most of the studies above presented quantum bit "qubit-based" computing in 2-dimensions. The limitations of today's technologies cause great challenges in obtaining both noise and information capacity in qubit-based computations.

Quantum digits ($d > 2$)—qudits are high-dimensional unit of quantum information. High-dimensional computation allows to store more information, reduce the complexity of the circuits used, increase the efficiency of the algorithms, and produce less noise [21, 22, 23]. The advantages that come with high dimension also boost the improvement of the application areas of quantum technology. For example, photon [24], nuclear magnetic resonance [25], ion trapped [26] based quantum computer types can also perform high-dimensional computation. Using these means of high dimension, Deutch-Jozsa, Berstein Vazirani, Grover Search Algorithm [21], Shor's algorithm [27] and multi-target Grover Search Algorithm [28] were adapted to high dimension. Further, the advantages of high dimension are also applicable to quantum key distribution devices [29, 30, 31, 32, 33, 34, 35]. Teleportation, which is one of the key techniques of quantum computing, has been adapted to high dimension too [36, 37, 38, 39, 40]. The Quantum Fourier Transform has been similarly adapted to high dimension [41, 42, 43]. The advantages of the high-dimensional computation are also evident in the calculation of the pi number.

The Quantum Phase Estimation (QPE) algorithm [44], which is significant for quantum computing such as Order finding [44], Shor's algorithm [19] for finding the prime factors, is used to estimate the phase of an eigenvector of a unitary operator. It has not been previously possible to acquire the digits of the pi number after the comma with high precision by using the QPE algorithm in 2-dimension systems [45, 46] due to the number of qubits are limited in the current quantum computer architecture. Different methods other than the QPE algorithm are used to approximate the pi number based on quantum computing [52, 53].

Our motivation in this work is to examine how effective the advantages of high-dimensional quantum computing will be in overcoming the difficulties in calculating pi with accuracy. In this study, we reveal that it is possible to reach the pi number with higher precision by using the $d$-dimensional QPE algorithms such as single and multi-global phase. The results obtained (please see Table 1) show that using high-dimensional quantum computing, the number pi can be calculated with both high precision and using less quantum resources. Also, all calculations are experimentally, implemented on Cirq [47].

This paper is outlined as follows: Section 2 presents the preliminaries and Section 3 and 4, respectively, offers the results of implementation with single and multi-global QPE algorithms used to estimate the pi number with high precision. Section 5 concludes with the comparison of the results of implementation by table. Some remarks are offered in Section 6.

## 2 Preliminaries

Qudits mathematically express a quantum state in the $d$-dimensional complex Hilbert space ($\mathcal{H}$) [48]. The orthonormal $d$-dimensional bases are as follows: $|f\rangle_d \in \{|0\rangle, |1\rangle, \ \dots \ , |d-1\rangle\}$. A $d$-dimensional quantum state is defined as below:

$$|\psi\rangle_d = \sum_{k=0}^{d-1} \alpha_k \, |k\rangle \in \mathcal{H}^d. \tag{1}$$

The eigenvalues of the vector $|\psi\rangle_d$ which describes this quantum state in $d$-dimension, are: $\alpha \in \{\alpha_0, \alpha_1, \ \dots \ , \alpha_{d-1}\}$. As the eigenvalues are considered as Gaussian probabilities in 2-dimension quantum systems, the eigenvalues must satisfy the equation that is the sum of their conjugate products:

$$\sum_{k=0}^{d-1} \alpha_k \, \alpha_k^* = 1. \tag{2}$$

Where $*$ refers complex conjugate. Unitary transformations, also known as the $d$-dimensional Weyl operators [49, 50], are expressed as follows:

$$\mathrm{U}_{pq}^d = \sum_{k=0}^{d-1} e^{\frac{2\pi i}{d} kp} \, |(k+q) \bmod d\rangle\langle k|, \quad p, q \in [0, \ d-1]. \tag{3}$$

Using Weyl operators, it is possible to obtain the high-dimensional equivalents of quantum transformations known in 2 dimension. As an illustration, the following matrices are used for the NOT (X) transformation in 3 dimension:

$$\mathrm{U}_{01}^3 = \mathrm{X} = \begin{pmatrix} 0 & 0 & 1 \\ 1 & 0 & 0 \\ 0 & 1 & 0 \end{pmatrix}, \qquad \mathrm{U}_{02}^3 = \mathrm{X}^2 = \begin{pmatrix} 0 & 1 & 0 \\ 0 & 0 & 1 \\ 1 & 0 & 0 \end{pmatrix}. \tag{4}$$

The general phase transformation required for the high-dimensional QPE (HD-QPE) algorithm used in this study is as follows in $d$-dimension:

$$diag(\mathrm{Z}^d) = (1, \ \omega, \ \omega^2, \ \dots, \ \omega^{d-1}), \tag{5}$$

where $\omega = e^{\frac{2\pi i}{d}}$. The $d$-dimensional formula of the effect of the Quantum General Fourier Transform (QGFT) algorithm used in this study on an $n$ qudit $|j\rangle$ state is as below:

$$\mathrm{F}(d, N)|j\rangle = \frac{1}{\sqrt{N}} \sum_{k=0}^{N-1} e^{\frac{2\pi i}{N} jk} |k_{(d)}\rangle, \quad N = d^n, \tag{6}$$

where $j \in \{0, N-1\}$ [42]. Using equation (6), it is possible to obtain the following generalized Hadamard transform, which is used to generate superposition in quantum computing when the number of qudits is $n = 1$:

$$\mathrm{H}^d|j\rangle = \mathrm{F}(d,d)|j\rangle = \frac{1}{\sqrt{d}}\sum_{k=0}^{d-1}\omega^{jk}|k\rangle. \tag{7}$$

## 3 Estimating pi number on *d*-dimensional using single-global QPE algorithm

Quantum computing makes it possible to calculate approximate values in quantum computers, similar to the behavior of numbers in modular arithmetic [51]. In the Hilbert-Schmidt space, when a phase transformation is applied to the qubits in superposition state, vector amplitudes are transformed into a series. These phase transformations, which are proportional to the amount of convergence, are achieved by successively applying quantum gates to the quantum state. Such calculations can be performed on quantum computers [45, 46, 52, 53].

The superior computational ability of quantum computers due to the superposition principle renders it possible to calculate the pi number, which is an irregular number, with higher precision. No previous study in the relevant literature has attempted to calculate the pi number in high dimension. Also, thanks to the advantages of high-dimension computing, approximation of the pi number is more advantageous in high-dimension than in the classical approach and the qubit-based approach.

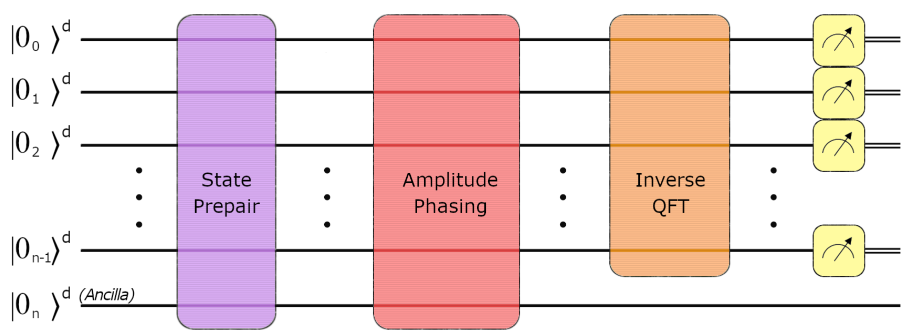


Fig. 1. High-dimensional QPE algorithm circuit used to converge to the pi number containing $n+1$ qudits in $d$-dimension.

The circuit with $n+1$ qudit in $d$-dimension, 1 of which is ancilla qudit, given in **Fig. 1**, contains the steps of state prepair, amplitude phasing, Inverse QFT and measurements. Using this circuit with the following initial state:

$$|\psi_{init}\rangle = |0\rangle_d^{\otimes n+1}, \tag{8}$$

the convergence algorithm to the pi number takes place in **V** steps.

**Step I (State Prepair):** Initially, using the generalized Hadamard gate obtained through the equation (7), the eigenvectors of $n$ qudits are converted into the superposition state with equal amplitude, and the ancilla qudit is put into to the $|\mathrm{Anc}\rangle_d = |1\rangle$ state using the gate

$\mathrm{U}_{01}^{d}$ given in the equation (4):

$$|\psi_{SP}\rangle = (\mathrm{H}^{d})^{\otimes n}\,\mathrm{U}_{01}^{d}\,|\psi_{init}\rangle = \frac{1}{\sqrt{N}}\sum_{k=0}^{N-1}|k_{(d)}\rangle\,|1\rangle. \tag{9}$$

**Step II (Amplitude Phasing):** This step involves using the global phase multiplier of the ancilla qudit to obtain a sequential series specific to the value of approximation to the quantum state amplitudes. The Amplitude Phasing (AP) transformation that must be calculated for approximation of the pi number in this step underlying the HD-QPE algorithm, is as follows:

$$\begin{array}{rl} {}^{m}\mathrm{AP}_{n+1}^{d} = diag( & 1, e^{0[m(d-1)+(1-s)]}, e^{0(d-1)+1}, e^{0(d-1)+2}, \ldots, e^{0(d-1)+(d-2)}, \\ & 1, e^{1[m(d-1)+(1-s)]}, e^{1(d-1)+1}, e^{1(d-1)+2}, \ldots, e^{1(d-1)+(d-2)}, \\ & \vdots, \quad \vdots, \quad \vdots, \quad \vdots, \quad \ddots, \quad \vdots, \\ & 1, e^{(n+1)[m(d-1)+(1-s)]}, e^{(n+1)(d-1)+1}, e^{(n+1)(d-1)+2}, \ldots, e^{(n+1)(d-1)+(d-2)}). \end{array} \tag{10}$$

When $m \in \{0\}$, this produces a single-global phase variant; when $m \in \{1\}$, this creates a multi-global phased variant. The decomposition of this transformation includes symmetrical repetitive Multi-valued Controlled Phase gates (MVCZ). These gates are the generalized form of conventional controlled gates that can perform multiple checks and apply quantum transformation on target qudits, and are shown on the circuit in the figure below:

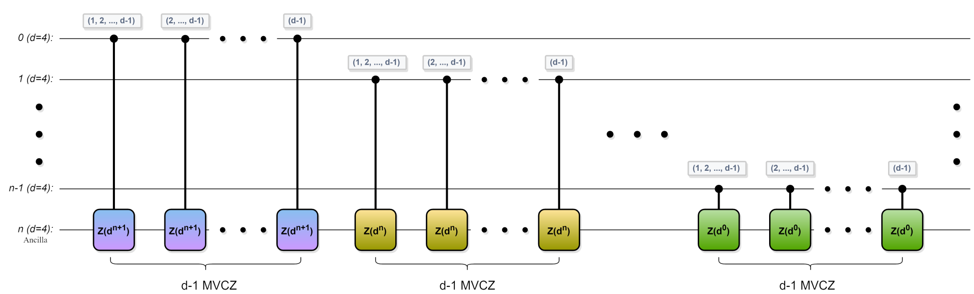


Fig. 2. The amount of conversion in radians and the position in the circuit of the MVCZ gates required for the approximation of the pi number, which forms the step of amplitude phasing for the $d$-dimension and $n$ qudits.

**Fig. 2** shows the sequential implementation of the MVCZ gates on the ancilla qudit. The index of the control qudit determines the number of the general phase gates that must be applied to the ancilla qudit, which is the target of these gates, in radians. At the end of this step, the quantum state expressing the sequential series in the phase space for the approximation of the pi number is as follows:

$$|\psi_{AP}\rangle = {}^{m}\mathrm{AP}_{n+1}^{d}\,|\psi_{SP}\rangle = \frac{1}{\sqrt{N}}\sum_{k=0}^{N-1} e^{k}|k_{(d)}\rangle\,|1\rangle, \quad m = 0 \text{ (for HD-QPE)}. \tag{11}$$

**Step III (Inverse QFT):** The Inverse Quantum Fourier Transform (IQFT) is a transform for calculating periods, as Shor [19] utilized in his prime factorization algorithm. This study outlines the period for the state $|\psi_{AP}\rangle$ using the generalized IQFT in $d$-dimension [21].

**Step IV (Measurements):** In $d$-dimension, the measurement operator measures the probability that a selected basis vector in the complex Hilbert space, as in the 2-dimension system, is found in areas equally divided by the number of dimensions. The positive-valued measurement operators in $d$-dimension are as follows: $POVM^d \in \{\prod_1, \prod_2, ..., \prod_N\}$ the measurement result of a qudit is in the range $[0,\ d-1]$. The measurements step of this study measures all the qudits $[0,\ n-1]$, except the ancilla qudit, based on this principle. This results in $M_{(d)}$, which refers to the countable period of the eigenvectors forming the quantum state.

**Step V (Post-processing):** In this study, the measurement results represent the period in the range of $[0,\ d^n) \in N$, which depends on the size and the number of qudits. The study performed in 2 dimensions obtains the equivalent of this period in the interval $[0, 1]$ through the calculation of the ratio of the period to the outcome space using the following equation [45]:

$$\theta = \frac{M_{10}}{d^n}. \tag{12}$$

Since $d^n$ is calculated in decimal base in equation (12), the change of base from $M_{(d)} = M_{(10)}$ is required at the end of the measurement. As can be seen in equation (12), $\theta$ is inversely proportional to $d^n$. Since the measurement result $M_{(d)}$ represents the period of one complete revolution on the unit circle in the phase space, the angular frequency $w = 2\pi\theta \simeq 1$ must be satisfied. Through this equation, the following equation expressing the approximation of the pi number is obtained:

$$\pi \simeq \frac{1}{2\theta}. \tag{13}$$

The implementation of the quantum circuit required for the approximation of the pi number with $d = 4$ dimensions and $n = 4$ qudits, using the HD-QPE algorithm, on Cirq is shown in the figure below.

Using the result of $M_{10} = 41$ obtained in **Fig. 3(b)**, the value of approximation to the pi number is acquired from the following calculation:

$$\theta = \frac{41}{4^4} = 0.16015625, \quad \pi \simeq \frac{1}{2\theta} = 3.12195121951. \tag{14}$$

The figure below presents the approximation errors at the logarithmic scale level related to the solution of the approximation of the pi number through the HD-QPE algorithm for $n = 4, 5, 6$ qudits by different dimensions.

As can be seen from **Fig. 4**, as the number of dimensions increases, the precision at which the approximation of the pi number is performed increases. For example, the implementation result (blue-colored line) with $n = 6$ qudits shows that a consistent approximation can be obtained to the pi number in 2 dimensions up to 1 digit, and in 9 dimensions up to 4 digits.

## 4 Estimating pi number on $d$-dimensional using multi-global QPE algorithm

A quantum state in high dimension may have more than one global phase, unlike traditional 2-dimension systems. It is possible to rewrite equation (1) considering the phase eigenvalues

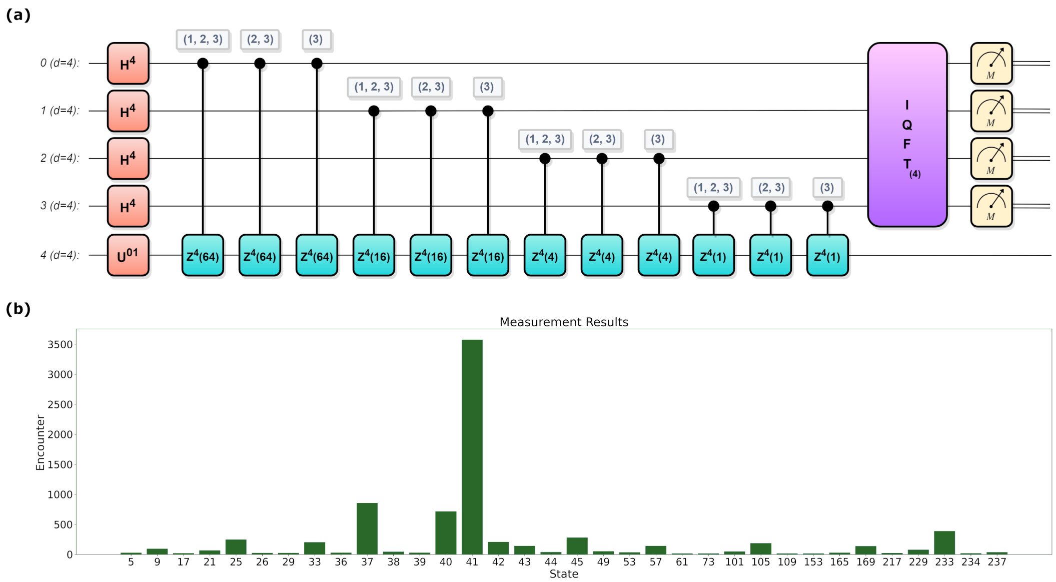


Fig. 3. **(a)** The approximation circuit of the pi number for $d = 4$ dimensions and $n = 4$ qudits using the HD-QPE algorithm. **(b)** The implementation result of the approximation of the pi number using the HD-QPE algorithm for $d = 4$-dimensional and $n = 4$ qudits (shot number is set 8192).

as follows [54]:

$$|\psi\rangle_d = \sum_{k=0}^{d-1} e^{\frac{2\pi i}{d}k}\,\alpha_k\,|k\rangle \in C. \tag{15}$$

Where $C$ refers set of complex numbers. As equation (15) shows, the eigenvalues of a qudit in $d$-dimension has $d-1$ global phase, factors. Activating these phases through the HD-QPE algorithm, one can obtain the multi-global QPE algorithm (HDM-QPE). Using the HDM-QPE, it is possible to make the approximation of the pi number with higher precision. To achieve this, if the following matrix transformation for the ancilla qudit, instead of $\mathrm{U}_{01}^{d}$, is employed in the step of state preparation:

$$\mathrm{AncGate}^d = \frac{1}{\sqrt{d-1}} \begin{pmatrix} 0 & 1 & 1 & 1 & \dots & 1 \\ 1 & 0 & 0 & 0 & \dots & 0 \\ 1 & 0 & 0 & 0 & \dots & 0 \\ 1 & 0 & 0 & 0 & \dots & 0 \\ \vdots & \vdots & \vdots & \vdots & \ddots & \vdots \\ 1 & 0 & 0 & 0 & \dots & 0 \end{pmatrix}, \tag{16}$$

the following state of the ancilla qudit for preparing the multi-global phases is obtained:

$$|\mathrm{Anc}\rangle = \frac{1}{\sqrt{d-1}} \sum_{k=1}^{d-1} |k\rangle. \tag{17}$$

This is an equal amplitude superposition state that does not contain only the $|0\rangle_d$ eigenvector. The resulting quantum state in equation (17) is in the following form, instead of equation (9)

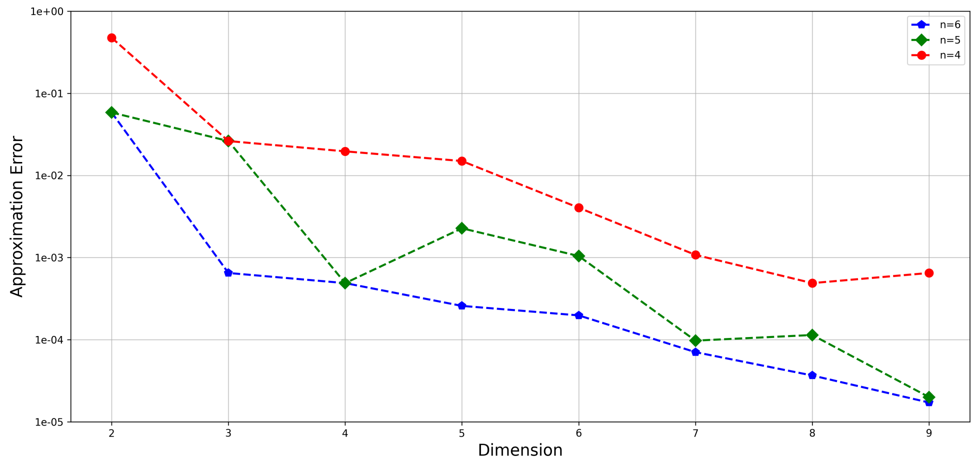


Fig. 4. The approximation errors at the logarithmic scale level related to the solution of the approximation of the pi number through the HD-QPE algorithm for $n = 4, 5, 6$ qudits by different dimensions.

in the HD-QPE:

$$|\psi_{SP}\rangle = (\mathrm{H}^d)^{\otimes n}\ \mathrm{AncGate}^d\ |\psi_{init}\rangle = \frac{1}{\sqrt{N}}\frac{1}{\sqrt{d-1}}\sum_{k=0}^{N-1}|k_{(d)}\rangle\,.\sum_{s=1}^{d-1}|s\rangle. \tag{18}$$

Another key difference in the multi-global phased method is that the amount of phases of the $\mathrm{MVCZ}^d$ gates applied to the ancilla qudit is $d-1$ times more. The resulting quantum state is expressed as follows instead of equation (11) in the HD-QPE:

$$|\psi_{AP}\rangle = {}^m\mathrm{AP}^d_{n+1}\,|\psi_{SP}\rangle = \frac{1}{\sqrt{N}}\frac{1}{\sqrt{d-1}}\sum_{k=0}^{N-1}e^{(d-1)k}\,|k_d\rangle\,.\sum_{s=1}^{d-1}e^{s}\,|s\rangle, \quad m = 1 \text{ (for HDM-QPE)}. \tag{19}$$

A second difference of the implementation in the HDM-QPE compared to the HD-QPE is that IQFT and measurement operator are applied to the ancilla qudit as well. Because of such measurement, the possible outcome space expands $d$ times. For this reason, the value $\theta$ in equation (12) must be recalculated in the step of post-processing using the following:

$$\theta = \frac{M_{10}}{d^{n+1}}. \tag{20}$$

Due to the expanding outcome space, the HDM-QPE implementation can perform approximation with at least equal to the pi number calculated or with higher precision using the equation (13) compared to the HD-QPE.

The figure below shows the quantum circuit required for the approximation of the pi number with $d = 4$ dimensions and $n = 4$ qudits, using the HDM-QPE algorithm on Cirq.

Based on the result obtained in **Fig. 5(b)**, $M_{10} = 163$, the approximate value of the pi number is obtained through the following calculation:

$$\theta = \frac{163}{4^5} = 0.1591796875, \quad \pi \simeq \frac{1}{2\theta} = 3.14110429448. \tag{21}$$

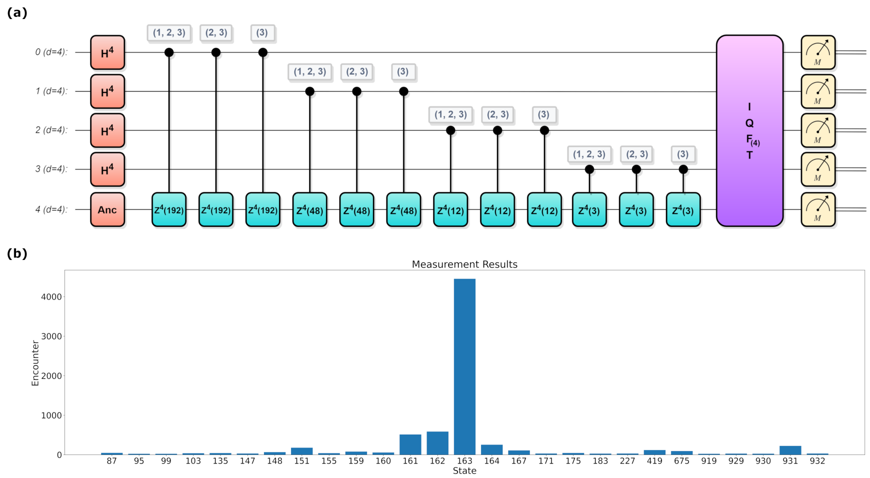


Fig. 5. **(a)** The circuit for the approximation of the pi number using multi-global phase for $d = 4$ dimensions and $n = 4$ qubits. **(b)** The result of the implementation of the approximation of the pi number using the HDM-QPE algorithm for $d = 4$ dimensions and $n = 4$ qubits (shot number is set 8192).

The figure below presents the approximation errors at the logarithmic scale level related to the solution of the approximation of the pi number in single and multi-global phases for $n = 4, 5, 6$ qudits by different dimensions.

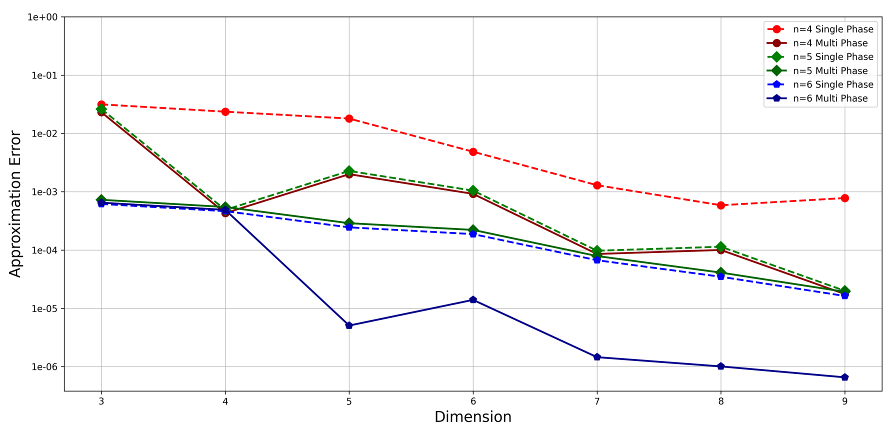


Fig. 6. Comparison of the approximation errors at the logarithmic scale level related to the approximation of the pi number obtained through the implementation of the HD-QPE and HDM-QPE algorithms for $n = 4, 5, 6$ qudits and $d = 3, \ldots, 9$ dimensions.

**Fig. 6** comparatively shows the error values on a logarithmic scale, where the pi number is approximated at least equal or higher precision while using the HDM-QPE algorithm, instead of the HD-QPE algorithm, when the number of qudits (or number of dimensions) is held constant. For example, the implementation of the HD-QPE algorithm for $n = 6$ qudits (the blue solid line) results in a consistent approach to the pi number by 4 digits for $d = 9$ dimensions, whereas the implementation of the the HDM-QPE algorithm results in a consistent approach to the pi number by 6 digits in the same dimension when applied on Cirq.

## 5 Discussion

The ability to store more information using less quantum resources and to have $d-1$ global phases in high-dimensional computing allows the QPE algorithm to be performed more efficiently. As the presence of $d-1$ global phases in the $d$-dimension allows better approximation to phase estimation in the QPE algorithm. That said, this study leverages the HD-QPE and HDM-QPE algorithms specifically to approximate the pi number with high precision in high-dimensional quantum computing.

Table 1. Results of the implementation of the pi number on Cirq[b] for $d = 2$ [45, 46] and $d = 3, \ldots, 9$ dimensions and different numbers of qudits. The number that represents the pi is considered to be pi = 3.1415926535897932 in the table.

| Dim ($d$) | Qudits($n$) | Single-phase $\|\epsilon\|$ | Multi-phase $\|\epsilon\|$ | Qudits($n$) | Single-phase $\|\epsilon\|$ | Multi-phase $\|\epsilon\|$ |
|---|---|---|---|---|---|---|
| | 3 | 4.000000000000000 | — | 8 | 3.121951219512195 | — |
| 2 | 4 | 2.666666666666667 | — | 9 | 3.160493827160493 | — |
| | 5 | 3.200000000000000 | — | 10 | 3.141104294478527 | — |
| | 6 | 3.200000000000000 | — | 11 | 3.141104294478527 | — |
| | 7 | 3.200000000000000 | — | 12 | 3.141104294478527 | — |
| | 3 | 3.375000000000000 | 3.115384615384615 | 8 | 3.142241379310344 | 3.141238429620172 |
| 3 | 4 | 3.115384615384615 | 3.115384615384615 | 9 | 3.141238429620172 | 3.141572675037241 |
| | 5 | 3.115384615384615 | 3.142241379310344 | 10 | 3.141572675037242 | 3.141572675037241 |
| | 6 | 3.142241379310344 | 3.142241379310344 | 11 | 3.141572675037242 | 3.141609817807781 |
| | 7 | 3.142241379310344 | 3.142241379310344 | 12 | 3.141609817807781 | 3.141597436786682 |
| | 3 | 3.200000000000000 | 3.121951219512195 | 8 | 3.141706615532118 | 3.141556013613920 |
| 4 | 4 | 3.121951219512195 | 3.141104294478527 | 9 | 3.141556013613920 | 3.141593662739834 |
| | 5 | 3.141104294478527 | 3.141104294478527 | 10 | 3.141593662739834 | 3.141593662739834 |
| | 6 | 3.141104294478527 | 3.141104294478527 | 11 | 3.141593662739834 | 3.141592486190990 |
| | 7 | 3.141104294478527 | 3.141706615532118 | 12 | 3.141592486190990 | 3.141592780328118 |
| | 3 | 3.125000000000000 | 3.156565656565656 | 8 | 3.141587582435258 | 3.141597688910049 |
| 5 | 4 | 3.156565656565656 | 3.143863179074446 | 9 | 3.141597688910049 | 3.141593646312330 |
| | 5 | 3.143863179074446 | 3.141334941696823 | 10 | 3.141593646312330 | 3.141592837794034 |
| | 6 | 3.141334941696823 | 3.141587582435258 | 11 | 3.141592837794034 | 3.141592676090425 |
| | 7 | 3.141587582435258 | 3.141587582435258 | 12 | 3.141592676090425 | 3.141592659920065 |
| | 3 | 3.176470588235293 | 3.145631067961165 | 8 | 3.141594873540601 | 3.141592914836509 |
| 6 | 4 | 3.145631067961164 | 3.140549273021001 | 9 | 3.141592914836509 | 3.141592588386064 |
| | 5 | 3.140549273021001 | 3.141395098303258 | 10 | 3.141592588386064 | 3.141592642794467 |
| | 6 | 3.141395098303259 | 3.141606625816443 | 11 | 3.141592642794467 | 3.141592651862534 |
| | 7 | 3.141606625816443 | 3.141594873540601 | 12 | 3.141592651862534 | 3.141592653373879 |
| | 3 | 3.118181818181818 | 3.142670157068062 | 8 | 3.141591198663320 | 3.141592666130632 |
| 7 | 4 | 3.142670157068062 | 3.141495327102803 | 9 | 3.141592666130632 | 3.141592666130632 |
| | 5 | 3.141495327102803 | 3.141663106173894 | 10 | 3.141592666130632 | 3.141592656147857 |
| | 6 | 3.141663106173894 | 3.141591198663319 | 11 | 3.141592656147857 | 3.141592653295635 |
| | 7 | 3.141591198663320 | 3.141591198663319 | 12 | 3.141592653295635 | 3.141592653499365 |
| | 3 | 3.160493827160493 | 3.141104294478527 | 7 | 3.141593662739834 | 3.141592486190990 |
| 8 | 4 | 3.141104294478527 | 3.141706615532118 | 8 | 3.141592486190990 | 3.141592633259547 |
| | 5 | 3.141706615532118 | 3.141556013613920 | 9 | 3.141592633259547 | 3.141592651643118 |
| | 6 | 3.141556013613920 | 3.141593662739834 | 10 | 3.141592651643118 | 3.141592653941064 |
| | 3 | 3.142241379310344 | 3.142241379310344 | 7 | 3.141593309801335 | 3.141592851248077 |
| 9 | 4 | 3.142241379310344 | 3.141572675037241 | 8 | 3.141592851248077 | 3.141592647446672 |
| | 5 | 3.141572675037242 | 3.141609817807781 | 9 | 3.141592647446672 | 3.141592653107822 |
| | 6 | 3.141609817807781 | 3.141593309801335 | 10 | 3.141592653107822 | 3.141592653736838 |

As **Table 1** shows, as the number of dimensions increases, the precision at which the approximation of the pi number can be performed increases. Also, when the number of the

[b] As there is no real quantum computer currently available that performs quantum computing in high dimension, the inability to compare the simulation results performed on Cirq with the results obtained by a real quantum computer seems to be a disadvantage.

single-global phase in the HD-QPE algorithm is increased to the multi-global phases and the number of qudits and dimensions is held constant, the approximation of the pi number takes place at least equal or higher precision on Cirq. Comparing equation (14) in the HD-QPE and equation (21) in the HDM-QPE, this study reveals that the HDM-QPE implementation achieves approximation of the pi number with higher consistency by 1 digit for the same number of dimensions and qudits. To illustrate in the table, the approximation of the pi number is consistently by 9 digits after the comma for $d = 9$ dimensions and $n = 9$ qudits, through the HDM-QPE algorithm. If we compare our results with the results of [45, 46] we have demonstrated that pi is approached equal or more precisely by using less quantum resources.

## 6 Conclusion

Quantum computing in high dimension has been attracting more and more attention these days thanks to its advantages including its ability to store more information using less qudits, to reduce the circuit complexity, to offer an increased efficiency of algorithms, and to reduce sensitivity to noise [21, 22, 23].

In this study, HD-QPE and HDM-QPE algorithms are implemented by using single and multi-global phase in $d$-dimension for estimating pi. This study concludes that pi can be approximated by using fewer quantum resources in high dimension with at least equal or higher precision than that obtained by 2-dimensional quantum computing. Also, when the number of qudits or the number of dimensions is kept constant, it is seen that the multi-global phase in high dimensions yields at least equal or better results than the single global phase. Lastly, proposed methods in this study which calculate the pi number with high precision may benefit the solutions of a lot of problems from cosmology to corrections in navigation to all sort of engineering problems, and so forth.

## Acknowledge

We sincerely appreciate the referees for their time in providing their valuable comments and suggestions, which allowed us to improve the quality of our paper.

## References

1. C. B. Boyer and U. C. Merzbach (2011), *A history of mathematics*, John Wiley & Sons.
2. H. H. Goldstine (2012), *A History of Numerical Analysis from the 16th through the 19th Century*, Springer Science & Business Media, Vol. 2.
3. T. J. Ypma (1995), *Historical development of the newton–raphson method*, SIAM review, 37(4):531–551.
4. S. Rao and A. W. Richa (2005), *New approximation techniques for some linear ordering problems*, SIAM Journal on Computing, 34(2):388–404.
5. W. F. Sheppard and H. Chisholm (1911), *Interpolation*, Encyclopædia Britannica, 14:706–710.
6. R. Y. Rubinstein and D. P. Kroese (2016), *Simulation and the Monte Carlo method*, John Wiley &Sons.
7. G. Fishman (2013), *Monte Carlo: concepts, algorithms, and applications*, Springer Science & Business Media.
8. D. P. Kroese, T. J. Brereton, T. Taimre and Z. I. Botev (2014), *Why the monte carlo method is so important today*, Wiley Interdisciplinary Reviews: Computational Statistics, 6, 2014.

9. C. Brezinski and L. Wuytack (2001), *Numerical analysis in the twentieth century. Numerical Analysis: Historical Developments in the 20th Century*, North–Holland, Amsterdam, pages 1–40.
10. P. Gawron, D. Kurzyk, and L. Pawela (2018), *Quantuminformation. jl?a julia package for numerical computation in quantum information theory*, PLoS One, 13(12):e0209358.
11. R. P. Feynman (2018), *Simulating physics with computers*, CRC Press, pages 133–153.
12. J. I. Cirac and P. Zoller (1995), *Quantum computations with cold trapped ions*, Physical review letters, 74(20):4091.
13. L. Vandersypen, M. Steffen, G. Breyta, C. Yannoni, M. Sherwood, and I. Chuang (2001), *Experimental realization of shor's quantum factoring algorithm using nuclear magnetic resonance*, Nature, 414:883–7, 12.
14. S. Khasminskaya, F. Pyatkov, K. Slowik, S. Ferrari, O. Kahl, V. Kovalyuk, P. Rath, A. Vetter, F. Hennrich, M. M. Kappes, et al (2016), *Fully integrated quantum photonic circuit with an electrically driven light source*, Nature Photonics, 10(11):727–732.
15. D. G. Cory, A. F. Fahmy, and T. F. Havel (1996), *Proceedings of the 4th workshop on physics and computation*, Boston, MA: New England Complex Systems Institute, page 87.
16. L. K. Grover (1996), *A fast quantum mechanical algorithm for database search*, In Proceedings of the twenty-eighth annual ACM symposium on Theory of computing, pages 212–219.
17. D. Deutsch (1985), *Quantum theory, the church–turing principle and the universal quantum computer*, Proceedings of the Royal Society of London. A. Mathematical and Physical Sciences, 400(1818):97–117.
18. D. Deutsch and R. Jozsa (1992), *Rapid solution of problems by quantum computation*, Proceedings of the Royal Society of London. Series A: Mathematical and Physical Sciences, 439(1907):553–558.
19. P. W. Shor (1999), *Polynomial-time algorithms for prime factorization and discrete logarithms on a quantum computer*, SIAM review, 41(2):303–332.
20. F. Arute, K. Arya, R. Babbush, D. Bacon, J. C. Bardin, R. Barends, R. Biswas, S. Boixo, F. GSL Brandao, D. A. Buell, et al (2019), *Quantum supremacy using a programmable superconducting processor*, Nature, 574(7779):505–510.
21. Y. Wang, Z. Hu, B. C. Sanders, and Sabre Kais (2020), *Qudits and high-dimensional quantum computing*, Frontiers in Physics, 8:589504.
22. M. Luo and X. Wang (2014), *Universal quantum computation with qudits*, Science China Physics, Mechanics and Astronomy, 57:1712–1717.
23. D. Cozzolino, B. D. Lio, D. Bacco, and L. K. Oxenløwe (2019), *High-dimensional quantum communication: benefits, progress, and future challenges*, Advanced Quantum Technologies, 2(12):1900038.
24. Y. Chi, J. Huang, Z. Zhang, J. Mao, Z. Zhou, X. Chen, C. Zhai, J. Bao, T. Dai, H. Yuan, et al (2022), *A programmable qudit-based quantum processor*, Nature communications, 13(1):1166.
25. Z. Gedik, I. Almeida Silva, B. Çakmak, G. Karpat, E. L. G. Vidoto, D. O. Soares-Pinto, E. R. deAzevedo, and F. F. Fanchini (2015), *Computational speed-up with a single qudit*, Scientific reports, 5(1):14671.
26. M. Ringbauer, M. Meth, L. Postler, R. Stricker, R. Blatt, P. Schindler, and T. Monz (2022), *A universal qudit quantum processor with trapped ions*, Nature Physics, 18(9):1053–1057.
27. A. Bocharov, M. Roetteler, and K. M. Svore (2017), *Factoring with qutrits: Shor's algorithm on ternary and metaplectic quantum architectures*, Physical Review A, 96(1):012306.
28. E. Acar, S. Gündüz, G. Akpınar, and İ. Yılmaz (2022), *High-dimensional grover multi-target search algorithm on cirq*, The European Physical Journal Plus, 137(2):1–9.
29. X. Yan, N. Zhou, L. Gong, Y. Wang, and X. Wen (2019), *High-dimensional quantum key distribution based on qudits transmission with quantum fourier transform*, Quantum Information Processing, 18:1–14.
30. C. Sekga, M. Mafu, and M. Senekane (2023), *High-dimensional quantum key distribution implemented with biphotons*, Scientific Reports, 13(1):1229.
31. T. Brougham, S. M. Barnett, K. T. McCusker, P. G. Kwiat, and D. J. Gauthier (2013), *Security of high-dimensional quantum key distribution protocols using franson interferometers*, Journal of

Physics B: Atomic, Molecular and Optical Physics, 46(10):104010.

32. S. Etcheverry, G. Canas, E. S. Gomez, W. A. T. Nogueira, C. Saavedra, G. B. Xavier, and G. Lima (2013), *Quantum key distribution session with 16-dimensional photonic states*, Scientific reports, 3(1):1–5.
33. I. Vagniluca, B. D. Lio, D. Rusca, D. Cozzolino, Y. Ding, H. Zbinden, A. Zavatta, L. K. Oxenløwe, and D. Bacco (2020), *Efficient time-bin encoding for practical high-dimensional quantum key distribution*, Physical Review Applied, 14(1):014051.
34. F. Bouchard, K. Heshami, D. England, R. Fickler, R. W. Boyd, B. G. Englert, L. L. Sanchez-Soto, and E. Karimi (2018), *Experimental investigation of high-dimensional quantum key distribution protocols with twisted photons*, Quantum, 2:111.
35. Y. Ding, D. Bacco, K. Dalgaard, X. Cai, X. Zhou, K. Rottwitt, and L. K. Oxenløwe. (2017), *High-dimensional quantum key distribution based on multicore fiber using silicon photonic integrated circuits*, NPJ Quantum Information, 3(1):25.
36. Y. Luo, H. Zhong, M. Erhard, X. Wang, L. Peng, M. Krenn, X. Jiang, L. Li, N. Liu, C. Lu, et al. (2019), *Quantum teleportation in high dimensions*, Physical review letters, 123(7):070505.
37. X. Hu, C. Zhang, B. Liu, Y. Cai, X. Ye, Y. Guo, W. Xing, C. Huang, Y. Huang, C. Li, et al. (2020), *Experimental high-dimensional quantum teleportation*, Physical Review Letters, 125(23):230501.
38. A. Fonseca (2019), *High-dimensional quantum teleportation under noisy environments*, Physical Review A, 100(6):062311.
39. W. Xu, T. Wang, and C. Wang (2019), *Efficient teleportation for high-dimensional quantum computing*, IEEE Access, 7:115331–115338.
40. Z. You-Bang (2007), *Controlled teleportation of high-dimension quantum-states with generalized bell-state measurement*, Chinese Physics, 16(9):2557.
41. H. Qin, R. Tso, and Y. Dai. (2018), *Multi-dimensional quantum state sharing based on quantum fourier transform*, Quantum Information Processing, 17:1–12.
42. Y. Cao, S. Peng, C. Zheng, and G. Long (2011), *Quantum fourier transform and phase estimation in qudit system*, Communications in Theoretical Physics, 55(5):790.
43. X. Fu, W. Bao, C. Zhou, and Z. Song (2012), *t-bit semiclassical quantum fourier transform*, Chinese Science Bulletin, 57:119–124.
44. M. A. Nielsen and I. L. Chuang (2001), *Quantum computation and quantum information*, Phys. Today, 54(2):60.
45. Qiskit, *Estimating pi using quantum phase estimation algorithm*, Nov 2022. (Last accessed: 04.04.2023).
46. H. H. Genç, S. Aydın, and H. Erdal (2020), *Yüksek hassasiyetli kayan nokta sayı hesaplamalarında bulut temelli kuantum bilgisayar programlama platformlarının kullanımı*, 4. ULUSLARARASI MARMARA FEN BİLİMLERİ KONGRESİ, Kocaeli, Turkey, 19 - 20 June 2020, vol.3, pp.387-397.
47. Cirq Developers (2022), *Cirq*, See full list of authors on Github: https://github.com/quantumlib/Cirq/graphs/contributors.
48. J. Brylinski. R. Brylinskir (2002), *Universal quantum gates*, Mathematics of quantum computation, 79.
49. J. Patera and H. Zassenhaus (1988), *The pauli matrices in n dimensions and finest gradings of simple lie algebras of type a n-1*, Journal of Mathematical Physics, 29(3):665–673.
50. M. Berkani (2007), *On the equivalence of weyl theorem and generalized weyl theorem*, Acta Mathematica Sinica, English series, 23:103–110.
51. S. Herbert (2022), *Quantum monte carlo integration: the full advantage in minimal circuit depth*, Quantum, 6:823.
52. T. Noto (2020), *Quantum circuit to estimate pi using quantum amplitude estimation*, arXiv preprint arXiv:2008.02623.
53. G. A. Bochkin, S. I. Doronin, E. B. Feldman, and A. I. Zenchuk (2020), *Calculation of $\pi$ on the ibm quantum computer and the accuracy of one-qubit operations*, Quantum Information Processing, 19(8):257.
54. B. Li, Z. Yu, and S. Fei ,*Geometry of quantum computation with qutrits*, Scientific reports, 3(1):1–6.